The Inversion of Bicyclobutane and Bicyclodiazoxane

Kiet A. Nguyen,† Mark S. Gordon,*,† and Jerry A. Boatz‡

Contribution from the Department of Chemistry, Iowa State University, Ames, Iowa 50011, and Phillips Laboratory, Olac PL/RKFE, Edwards Air Force Base, California 93523-5000

Received January 28, 1993®

Abstract: Multiconfigurational wave functions were used to study the inversion processes of bicyclobutane (C_4H_6) and its isoelectronic congener bicyclodiazoxane (N_2O_2). The barriers are about 50 (47) and 40 (32) kcal/mol, respectively, as calculated with multireference CI (second-order multireference perturbation theory). Multiconfigurational descriptions of these systems with simpler GVB wave functions were also carried out. Good agreement between GVB and MCSCF is obtained for geometries. The GVB energetics are not reliable, but relative energies obtained at GVB geometries, using higher levels of theory, provide a reasonable representation of the potential energy surface.

I. Introduction

In the presence of a proton source, such as an alcohol, bicyclobutane (**1**) can be produced from the thermal conversion of the anion derived from cyclopropanecarboxaldehyde tosylhydrazone.[1a] The irradiation of butadiene also produces bicyclobutane.[1b] The molecular and electronic structure of this compound[2] and the reactions[3] it can undergo have been the subject of both experimental and theoretical investigations. In particular, two competing processes that **1** can undergo are the inversion to an equivalent isomer and the isomerization to butadiene. This work is concerned with the former process.

An early paper related to bicyclobutane inversion was the two-configurational self-consistent field (TCSCF) calculation by Feller, Davidson, and Borden[3d] on dimethylenebicyclobutane, using the STO-3G basis set.[4] These authors verified the planar structure of the transition state by diagonalizing the matrix of energy second derivatives (Hessian) and demonstrating that this matrix has just one negative eigenvalue. They found significant mixing at the transition state between the ...a_1^2 and ...b_1^2 configurations, where the a_1 and b_1 orbitals are the highest occupied (HOMO) and lowest unoccupied (LUMO) in the SCF configuration.

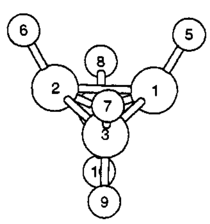

1 (C_{2v})

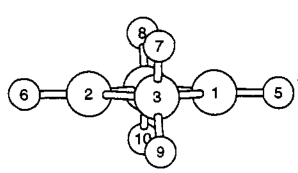

2 (D_{2h})

The first calculation of the inversion of bicyclobutane was done by Gassman and co-workers[3b] using one pair [GVB-P(1)] generalized valence bond[5] wave functions (equivalent to the TCSCF wave function) within the PRDDO approximation.[6] An analysis of the inversion potential energy surface (PES) suggested that the transition state structure has C_{2v} symmetry, such that the bridgehead hydrogens are out of the plane of the four carbons, leading to a 30 kcal/mol "barrier", in agreement with the experimental value (26 kcal/mol) for a substituted compound in which the bridgehead (H_5 and H_6) and two of four peripheral (H_9 and H_{10}, or H_7 and H_8) hydrogens are replaced with phenyl (C_5H_6) and methanecarboxylate groups, respectively.[7] The C_{2v} structure was found to be 4 kcal/mol lower in energy than the planar D_{2h} **2** structure; however, the Hessian was not calculated to verify that the C_{2v} structure is indeed a transition state. The bridgehead C–C bond length at the C_{2v} structure was predicted to be 2.017 Å, leading to significant diradical character. Even though the proposed transition structure has C_{2v} symmetry, the authors suggested that the inversion requires motion through a planar D_{2h} **2** structure.

Schleyer and co-workers[8] also considered bicyclobutane with GVB-P(1) wave functions, using the 3-21G basis set;[9] however, only the minimum and D_{2h} structures were examined. No Hessian calculations were performed, since the authors asserted that the inversion motion must go through the D_{2h} structure. The latter structure is predicted to have a C–C bridgehead distance of 2.103 Å and significant diradical character. The predicted SCF and GVB "barriers" are 90 and 30 kcal/mol, respectively.

The most recent theoretical study of bicyclobutane inversion was performed by Collins, Dutter, and Rauk (CDR)[10b] with restricted Hartree–Fock (RHF) wave functions and the 6-31G(d) basis set.[11] The authors verified their D_{2h} **2** transition state by diagonalizing the Hessian. Their MP3/6-31G(d)[12] barrier at the RHF geometry is 82.4 kcal/mol (including zero point energy

† Iowa State University.
‡ Edwards Air Force Base.
® Abstract published in *Advance ACS Abstracts*, September 1, 1994.

(1) (a) Wiberg, K. B.; Lavanish, J. M. *J. Am. Chem. Soc.* **1966**, *88*, 365. (b) Srinivasan, R.; Levi, A. A.; Haller, I. *J. Phys. Chem.* **1969**, *69*, 1775.
(2) Pomerantz, M.; Abrahamson, E. W. *J. Am. Chem. Soc.* **1966**, *88*, 3970.
(3) (a) Wiberg, K. G. J. *J. Am. Chem. Soc.* **1983**, *105*, 1227. (b) Gassman, P. G.; Greenlee, M. L.; Dixon, D. A.; Richtsmeier, S.; Gougoutas, J. Z. J. *J. Am. Chem. Soc.* **1983**, *105*, 5865. (c) Wiberg, K. B.; Bonneville, G.; Dempsey, R. *Isr. J. Chem.* **1983**, *23*, 85. (d) Golberg, A. H.; Doherty, D. H. *J. Am. Chem. Soc.* **1983**, *105*, 284. (e) Feller, D.; Davidson, E. R.; Borden, W. T. *J. Am. Chem. Soc.* **1982**, *104*, 1216.
(4) Hehre, W. J.; Stewart, R. F.; Pople, J. A. *J. Chem. Phys.* **1969**, *51*, 2657.
(5) Goddard, W. A., III; Dunning, T. H.; Hunt, W. J.; Hay, P. J. *Acc. Chem. Res.* **1973**, *6*, 368.
(6) Halgren, T. A.; Lipscomb, W. N. *J. Chem. Phys.* **1973**, *58*, 1569.
(7) (a) D'Yakanov, I. A.; Razen, V. V.; Komendantov, M. I. *Tetrahedron Lett.* **1966**, 1127, 1135. (b) Woodward, R. B.; Dalrymple, D. L. *J. Am. Chem. Soc.* **1969**, *91*, 4612.
(8) Budzelaar, P. H. M.; Kraka, E.; Cremer, D.; Schleyer, P. v. R. *J. Am. Chem. Soc.* **1986**, *108*, 561.
(9) (a) Binkley, J. S.; Pople, J. A.; Hehre, W. J. *J. Am. Chem. Soc.* **1980**, *102*, 1980. (b) Gordon, M. S.; Binkley, J. S.; Pople, J. A.; Pietro, W. J.; Hehre, W. J. *J. Chem. Phys.* **1982**, *104*, 2997.
(10) (a) Wiberg, K. B.; Bader, R. F. W.; Lau, C. D. H. *J. Am. Chem. Soc.* **1987**, *109*, 985, 1001. (b) Politzer, P.; Kirschenheuter, G. P.; Alster, J. *J. Am. Chem. Soc.* **1987**, *106*, 4211. (c) Collins, S.; Dutler, R.; Rauk, A. *J. Am. Chem. Soc.* **1987**, *109*, 2564. (d) Walters, V. A.; Hadad, C. M.; Thiel, Y.; Colson, S. D.; Wiberg, K. B.; Johnson, P. M.; Foresman, J. B. *J. Am. Chem. Soc.* **1991**, *113*, 4782.
(11) (a) Hariharan, P. C.; Pople, J. A. *Theor. Chim. Acta* **1973**, *28*, 213. (b) Gordon, M. S. *Phys. Lett.* **1980**, *76*, 2997.
(12) Krishnan, R.; Frisch, M. J.; Pople, J. A. *J. Chem. Phys.* **1980**, *72*, 4244.

0002-7863/94/1516-9241$04.50/0

corrections), similar to the RHF value obtained by Schleyer and co-workers. A configuration interaction calculation including all single and double excitation (CISD) gave essentially the same result. The authors attributed the disparity between their results and those from experiment to either substituent effects or the triplet state playing a role in the inversion process.

Very recently, bicyclodiazoxane (**3**), an isoelectronic analog of bicyclobutane, has been suggested as a possible high energy density (HEDM) material,[13] based on calculations using both SCF and GVB wave functions with the 6-31G(d) basis set. Although recent experiments by Wodtke and co-workers[14,15] have inferred the possible existence of **3** and its bond stretch isomer **4** as well as other N_2O_2 isomers, little is known about bicyclodiazoxane.

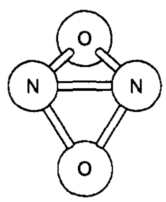

3 C_{2v}

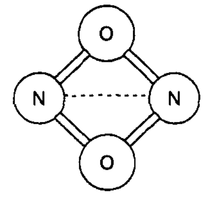

4 D_{2h}

In the present study, the inversion process of both bicyclobutane and bicyclodiazoxane will be examined in detail at several levels of theory using multiconfigurational wave functions.

II. Methods of Calculation

Several levels of multiconfigurational wave function have been used in this work. The active space for the TCSCF calculations consisted of the HOMO and LUMO in the SCF configuration, corresponding to the bridgehead bonding and antibonding (N–N or C–C σ and σ^*) orbitals. This is the smallest reference space required to ensure a proper qualitative description of species having large biradical character, as in the case of structures in the transition state region of the bicyclobutane inversion.[3d,b,8] To quantitatively account for the changes in the bicyclobutane and bicyclodiazoxane rings upon inversion, the reference space is expanded by combining five doubly occupied bonding MOs and their corresponding antibonding MOs, creating the five perfect pairs GVB [GVB-P(5)] wave function and 19404 spin adapted configuration state functions (CFS) making up the 10 orbitals and 10 electrons MCSCF [MCSCF(10,10)] wave function. These 10 active orbitals correspond to (1) five C–C bonding and antibonding MOs of bicyclobutane and (2) one N–N and four N–O bonding and antibonding MOs of bicyclodiazoxane. The GVB-P(5) wave function ignores interactions between correlated pairs. These interactions are included in the full MCSCF(10,10) or CASSCF(10,10) wave function.

The multiconfigurational description of geometries and energetics evaluated with TCSCF, multiple pair generalized valence bond[5] (GVB) and fully optimized reaction space (FORS) MCSCF[16] wave functions were calculated using the GAMESS[17] quantum chemistry program system. Structures were obtained with the use of the analytically determined gradients. Minima and transition states were verified by evaluating the appropriate matrix of energy second derivatives (hessian) from finite differences of the analytically determined gradients. TCSCF Hessians were evaluated analytically. The final energies were obtained by performing single internally contracted multireference CI (MRCI)[18] calculations (including all single and double excitations from the active orbitals of the MCSCF(10,10) reference space), using the MCSCF(10,10) wave functions to define the reference space [MRCI(10,10)//MCSCF(10,10)]. It has been demonstrated that internally contracted MRCI calculations are in close agreement with the corresponding uncontracted or second-order CI (SOCI) results.[18] MRCI calculations were done using the MOLPRO[18] codes.

In addition, second-order perturbation theory calculations with the CASSCF(10,10) wave function as the reference space (PT2) were also carried out to assess the effect of dynamic electron correlation that is not included in the MRCI(10,10). PT2[19] calculations of two different types of Møller–Plesset-like partitioning were carried out using the MOLCAS-2 program.[20] The PT2D partitioning includes only the diagonal part of the one-electron operator in the zeroth-order Hamiltonian while PT2F also includes all non-diagonal elements. Only the former is invariant to orbital transformations. PT2F has been shown to give accurate energetics for a number of systems containing first-row atoms.[21]

In order to properly connect each transition state with its corresponding minima on the potential energy surface, minimum energy paths (MEP) were traced by following the paths of steepest descents in mass-weighted Cartesian coordinates[22,23] using the concept of intrinsic reaction coordinate[22,24] (IRC). The reaction paths (MEPs) were generated using the second-order Gonzalez–Schlegel (GS2)[25] method encoded in GAMESS.[17] The initial step off the saddle point was taken by following the imaginary normal mode with a 0.12 amu$^{1/2}$ bohr step. Other points on the MEP were located with a step size of 0.17 amu$^{1/2}$ bohr (Δs = 0.17 amu$^{1/2}$ bohr).

All geometry searches and IRC calculations were done with the 6-31G(d) basis set.[11] MRCI and CASPT2 calculations were carried out using the 6-31G(d),[11] 6-311G(d,p),[26] and 6-311+G(2d)[27] basis sets.

III. Results and Discussion

1. Bicyclobutane. The two central issues to be resolved are the nature of the inversion transition state(s) and the height of the inversion barrier. Consequently, initial calculations focused on structures **1** and **2**, starting with the structural and bonding issues. The C_{2v} structure **1** is verified to be a minimum on the bicyclobutane PES by its positive definite Hessian at three different levels of theory, GVB-P(1), GVB-P(5), and MCSCF(10,10), using the 6-31G(d) basis set. The C–C bond distances obtained at all three leels of theory compare favorably with the experimentally determined bridgehead C_1–C_2 and peripheral C_1–C_3 bond distances of 1.497 and 1.498 Å, respectively (see Table 1).[28] Our highest correlated level of theory [MCSCF(10,10)/

(13) Gordon, M. S.; Windus, T. L.; Nguyen, K. A.; Matsunaga, N. Potential Energy Surfaces and Dynamics of Potential HEDM Molecules. In *Proceedings of The High Energy Density Materials Contractors Conference*; AFOSR: Washington, DC, 1991.

(14) Yang, X.; Kim, E. H.; Wodtke, A. M. *J. Chem. Phys.* **1992**, *96*, 5111.

(15) Yang, X.; Price, J. M.; Mack, J. A.; Morgan, C. G.; Rogaski, C. A.; McGuire, D. X.; Kim, E. H.; Wodtke, A. M. *J. Phys. Chem.* **1993**, *97*, 3944.

(16) (a) Lengsfield, B. H., III *J. Chem. Phys.* **1980**, *73*, 382. (b) Jarkony, D. R. *Chem. Phys. Lett.* **1981**, *77*, 634. (c) Ruedenberg, K.; Schmidt, M. W.; Dombek, M. M.; Elbert, S. T. *Chem. Phys.* **1982**, *71*, 41, 51, 65. (d) Lam, B.; Schmidt, M. W.; Ruedenberg, K. *J. Phys. Chem.* **1985**, *89*, 2221. (e) Werner, H.-J.; Knowles, P. J. *J. Chem. Phys.* **1985**, *82*, 5053. (f) Werner, H.-J.; Knowles, P. J. *Chem. Phys. Lett.* **1985**, *115*, 259.

(17) GAMESS (General Atomic and Molecular Electronic Structure System): (a) Schmidt, M. W.; Baldridge, K. K.; Boatz, J. A.; Jensen, J. H.; Koseki, S.; Gordon, M. S.; Nguyen, K. A.; Windus, T. L.; Elbert, S. T. *QCPE Bull.* **1990**, *10*, 52. (b) Schmidt, M. W.; Baldridge, K. K.; Boatz, J. A.; Elbert, S. T.; Gordon, M. S.; Jensen, J. H.; Koseki, S.; Matsunaga, N.; Nguyen, K. A.; Su, S.; Windus, T. L. *J. Comp. Chem.* **1993**, *14*, 1347.

(18) (a) Werner, H.-J.; Knowles, P. J. *J. Chem. Phys.* **1988**, *89*, 5803. (b) Werner, H.-J.; Knowles, P. J. *Chem. Phys. Lett.* **1988**, *145*, 514. MOLPRO is written by Werner, H.-J.; Knowles, P. J. with contributions by Almlöf, J.; Amos, R. D.; Elbert, S. T.; Taylor, P. R.

(19) (a) Anderson, K.; Malmqvist, P.-A.; Roos, B. O. *J. Chem. Phys.* **1992**, *96*, 1218. (b) Anderson, K.; Malmqvist, P.-A.; Roos, B. O. *J. Phys. Chem.* **1990**, *94*, 5483.

(20) Anderson, K.; Fülscher, M. P.; Lindh, R.; Malmqvist, P.-A.; Olsen, J.; Roos, B. O.; Sadlej, A. J.; Wilmark, P.-O. MOLCAS Version 2, *User's Guide*; University of Lund; Sweden, 1991.

(21) (a) Anderson, K.; Roos, B. O. *Int. J. Quantum Chem.* **1993**, *45*, 591. (b) Serrano-Andres, L.; Merchan, M.; Nebot-Gil, I.; Roos, B. O.; Fülscher, M. *J. Am. Chem. Soc.* **1993**, *115*, 6184. (c) Borowski, B.; Anderson, K.; Malmqvist, P.-A.; Roos, B. O. *J. Chem. Phys.* **1992**, *97*, 5569. (d) Anderson, K.; Roos, B. O. *Chem. Phys. Lett.* **1992**, *191*, 507. (e) Serrano-Andres, L.; Merchan, M.; Fülscher, M.; Roos, B. O. *Chem. Phys. Lett.* **1993**, *211*, 125.

(22) (a) Fukui, K. *Acc. Chem. Res.* **1981**, *14*, 363. (b) Fukui, K. *Pure Appl. Chem.* **1982**, *54*, 1825. (c) Fukui, K. *Int. J. Quantum Chem. Symp.* **1981**, *15*, 633.

(23) (a) Marcus, R. A. *J. Chem. Phys.* **1966**, *45*, 4493. (b) Marcus, R. A. *J. Chem. Phys.* **1968**, *49*, 2610. (c) Truhlar, D. G.; Kuperman, A. *J. Am. Chem. Soc.* **1971**, *93*, 1840. (d) Schaefer, H. F., III *Chem. Br.* **1975**, *11*, 227.

(24) (a) Ishida, K.; Morokuma, K.; Komornicki, A. *J. Chem. Phys.* **1977**, *66*, 2153. (b) Muller, K. *Angew. Chem., Int. Ed. Engl.* **1980**, *19*, 1. (c) Schmidt, M. W.; Gordon, M. S.; Dupuis, M. *J. Am. Chem. Soc.* **1985**, *107*, 2585. (d) Garrett, B. C.; Redmon, M. J.; Steckler, R.; Truhlar, D. G.; Baldrige, K. K.; Bartol, D.; Schmidt, M. W.; Gordon, M. S. *J. Phys. Chem.* **1988**, *92*, 1476.

(25) Gonzalez, C.; Schlegel, H. B. *J. Chem. Phys.* **1989**, *90*, 2154; *J. Phys. Chem.* **1990**, *94*, 2154; *J. Chem. Phys.* **1991**, *90*, 5853.

(26) (a) Krishnan, R.; Binkley, J. S.; Seeger, R.; Pople, J. A. *J. Chem. Phys.* **1980**, *72*, 650. (b) Clark, T.; Chandrasekhar, J.; Spitznagel, G. W.; Schleyer, P. von R. *J. Comput. Chem.* **1983**, *4*, 294.

(27) Frish, M. J.; Pople, J. A.; Binkley, J. S. *J. Chem. Phys.* **1984**, *80*, 3265.

(28) (a) Cox, K. W.; Harmony, M. D.; Nelson, G.; Wiberg, K. G. *J. Phys. Chem.* **1969**, *50*, 5107. (b) Cox, K. W.; Harmony, M. D.; Nelson, G.; Wiberg, K. G. *J. Phys. Chem.* **1970**, *53*, 858.

Table 1. MCSCF(10,10), GVB-P(5) (in parentheses) and GVP-P(1) (in brackets) Geometrical Parameters of C_4H_6 Systems, Calculated with the 6-31G(d) Basis Set

systems	**1**[a] (C_{2v})	**2**[b] (D_{2h})	**5**[a] (C_{2h})	**6**[c] (C_s)
		Bond distances (Å)		
C_1C_2	**1.521**	**2.088**	**2.168**	**2.113**
	(1.485)	(2.092)	(2.147)	(2.110)
	[1.504]	[2.059]	[2.121]	[2.079]
C_1C_3	**1.519**	**1.555**	**1.555**	**1.553**
	(1.516)	(1.542)	(1.546)	(1.548)
	[1.485]	[1.519]	[1.524]	[1.525]
H_5C_1	**1.069**	**1.073**	**1.078**	**1.074**
	(1.071)	(1.072)	(1.076)	(1.074)
	[1.070]	[1.072]	[1.078]	[1.075]
H_7C_3	**1.078**	**1.087**	**1.085**	**1.087**
	(1.079)	(1.088)	(1.086)	(1.089)
	[1.079]	[1.089]	[1.087]	[1.089]
H_9C_3	**1.080**	**1.087**	**1.085**	**1.087**
	(1.082)	(1.088)	(1.086)	(1.087)
	[1.082]	[1.089]	[1.087]	[1.088]
		Bond Angles (deg)		
$H_5C_1C_3$	**129.7**	**132.3**	**122.7**	**130.0**
	(131.0)	(132.7)	(126.2)	(128.7)
	[130.0]	[132.7]	[124.3]	[128.2]
$H_7C_3C_1$	**116.6**	**115.6**	**113.5**	**115.6**
	(116.6)	(115.5)	(114.8)	(115.4)
	[117.0]	[115.7]	[114.3]	[115.5]
$H_9C_3C_1$	**119.2**	**115.6**	**113.5**	**114.8**
	(120.1)	(115.5)	(114.8)	(114.9)
	[119.3]	[115.7]	[115.5]	[115.1]
		Dihedral Angles (deg)		
$C_4C_1C_2C_3$	**122.1**	**180.0**	**180.0**	**179.8**
	(119.4)	(180.0)	(180.0)	(178.4)
	[122.4]	[180.0]	[180.0]	[178.6]

[a] A minimum at all levels of theory. [b] MCSCF(10,10): a transition state. GVB-P(1) and GVB-P(5): two imaginary frequencies. [c] A transition state at all levels of theory. Distances: C_2C_3 = **1.550** (1.540) [1.516], H_6C_2 = **1.073** (1.072) [1.072]; Angles: $H_6C_2C_1$ = **131.6** (132.7) [132.8], $H_7C_3C_2$ = **114.8** (114.9) [115.2], $H_7C_3C_2$ = **114.9** (116.0) [116.1].

6-31G(d)] overestimates the bridgehead and peripheral C_1–C_3 distances by 0.024 and 0.021 Å, respectively. Since there is little configurational mixing at this geometry, good agreement with geometries predicted by earlier RHF and MP2 calculations is also obtained.[10c,d]

At all levels of theory the D_{2h} structure **2** is predicted to have a C_1–C_3 bridgehead distance greater than 2 Å. Although the three levels of theory agree in their prediction of bond distances and bond angles for structure **2** to within 0.03 Å and 0.5°, respectively, MCSCF(10,10) finds **2** to be a transition state with one 346i cm^{-1} imaginary frequency, while GVB-P(1) and GVB-P(5) incorrectly predict **2** to have two imaginary frequencies. The normal mode corresponding to the imaginary frequency at the MCSCF(10,10) transition state is displayed in Figure 1a. The small MCSCF(10,10) imaginary frequency (cf. 829i cm^{-1} obtained by RHF with the same basis set[10c]) signifies a wide potential barrier as verified by IRC calculations (see Figure 2a).

The IRC was traced from **2** to **1** by following the path of steepest descents starting at the transition state (**2**). These IRC calculations verify that the D_{2h} transition state (**2**), indeed, connects with the reactant (**1**). Figure 2a displays structures along the IRC to illustrate the structural rearrangement in the inversion process. Near the transition state, the IRC is quite flat (as expected from the small imaginary frequency) and involves mostly the bending of the bridgehead hydrogens. In fact, as the molecule proceeds from the transition state (**2**) through 33 steps on the IRC, with the two bridgehead hydrogens simultaneously bending to an H_5–C_1–C_2 angle of 11.2°, the energy drops only to 2.3 kcal/mol below the transition state (**2**). The remainder of the MEP involves bending of the bridgehead hydrogens as well as the peripheral carbons. Energetically, the MCSCF(10,10)/6-31G(d) inversion transition state (**2**) is 46.8 kcal/mol (with zero point corrections included) above bicyclobutane (**1**) (see Table 2). A single point correction with MRCI(10,10)/6-31G(d) and PT2F/6-31G(d) increases this barrier only slightly to

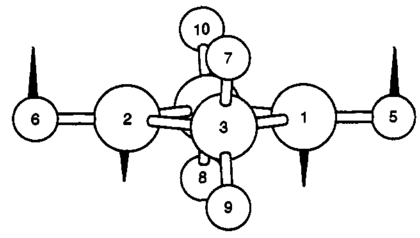

2

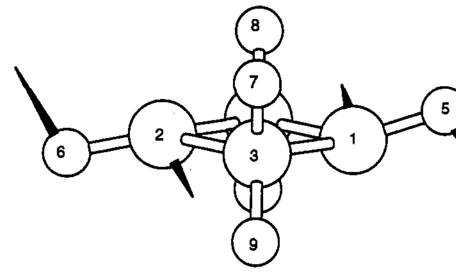

6

Figure 1. (a, top) MCSCF(10,10)/6-31G(d) imaginary normal mode (346i cm^{-1}) for **2**. (b, bottom) MCSCF(10,10)/6-31G(d) imaginary normal mode (280i cm^{-1}) for **6**.

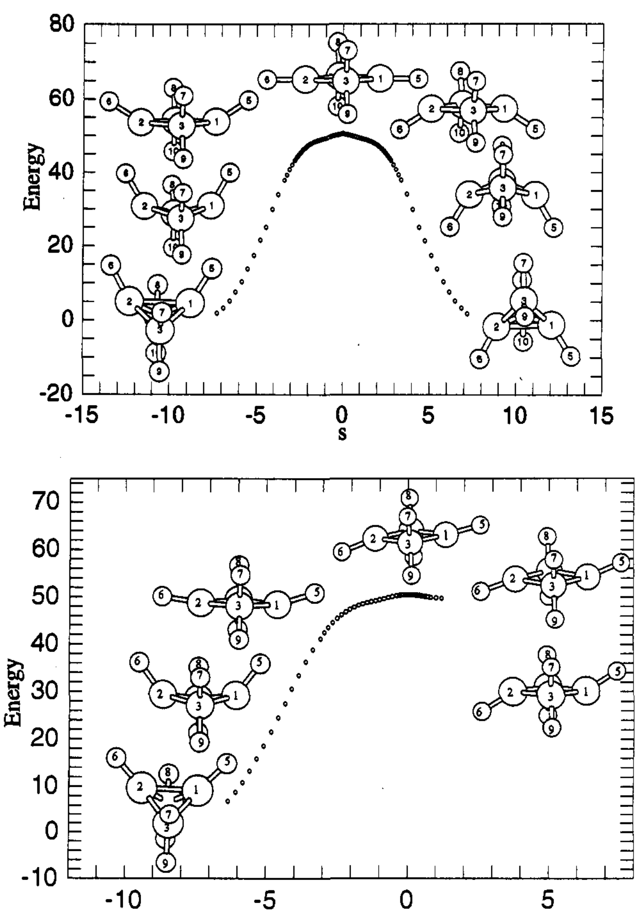

Figure 2. (a, top) Inversion IRC of bicyclobutane calculated with MCSCF(10,10)/6-31G(d); energy in kcal/mol, s in amu$^{1/2}$·bohr. The structures displayed along the IRC are for the transition state **2** (top) and for points 33, 66, and 72 for the forward ($s > 0$) and backward ($s < 0$) directions. (b, bottom) Bond stretch IRC of bicyclobutane, calculated with MCSCF(10,10)/6-31G(d); energy in kcal/mol, s in amu$^{1/2}$·bohr. The structures displayed along the IRC are of the transition state **6** (top); forward ($s > 0$), points 2 and 10; backward ($s < 0$), points 10, 20, and 30.

Table 2. 6-31G(d) Total (au) and Relative Energies (kcal/mol^{-1}) of C_4H_6 Structures[a]

systems	wave function	total energies	relative energies ΔE	relative energies ΔH_0[b]
1	GVB-P(1)//GVB-P(1)[c]	−154.888 32 (57.6)	0.0	0.0
	GVB-P(5)//GVB-P(5)[c]	−154.948 73 (57.2)	0.0	0.0
	MCSCF(10,10)//GVB-P(5)	−154.988 23	0.0	0.0
	MCSCF(10,10)//MCSCF(10,10)[c]	−154.989 04 (57.0)	0.0	0.0
	MRCI(10,10)//MCSCF(10,10)	−155.11561	0.0	0.0
	PT2F//MCSCF(10,10)	−155.41188	0.0	0.0
2	GVB-P(1)//GVB-P(1)[d]	−154.82383 (54.0)	40.5	36.9
	GVB-P(5)//GVB-P(5)[d]	−154.88526 (53.3)	39.8	35.9
	MCSCF(10,10)//GVB-P(5)	−154.90852	50.0	46.1
	MCSCF(10,10)//MCSCF(10,10)[e]	−154.90874 (53.4)	50.4	46.8
	MRCI(10,10)//MCSCF(10,10)	−155.02990	53.8	50.2
	PT2F//MCSCF(10,10)	−155.32929	51.8	48.2
5	GVB-P(1)//GVB-P(1)[c]	−154.82613 (55.6)	39.0	37.0
	GVB-P(5)//GVB-P(5)[c]	−154.88676 (54.7)	38.9	36.4
	MCSCF(10,10)//GVB-P(5)	−154.90928	49.5	47.0
	MCSCF(10,10)//MCSCF(10,10)[c]	−154.90976 (54.6)	49.7	47.3
	MRCI(10,10)//MCSCF(10,10)	−155.02934	54.1	51.7
	PT2F//MCSCF(10,10)	−155.32864	52.2	49.8
6	GVB-P(1)//GVB-P(1)[e]	−154.82452 (54.7)	40.0	37.1
	GVB-P(5)//GVB-P(5)[e]	−154.88580 (54.0)	39.5	36.3
	MCSCF(10,10)//GVB-P(5)	−154.49452	51.3	47.8
	MCSCF(10,10)//MCSCF(10,10)[e]	−154.908858 (53.5)	50.5	47.0
	MRCI(10,10)//MCSCF(10,10)	−155.02914	54.3	50.8
	PT2F//MCSCF(10,10)	−155.32897	52.2	48.5

[a] Zero point energies in parentheses. [b] Including zero point vibrational energies. [c] Minimum. [d] Two imaginary frequencies. [e] Transition state.

Table 3. 6†311G(d,p) Total (au) and Relative Energies (kcal/mol^{-1}) of the MCSCF(10,10)/6-31G(d) C_4H_6 Structures

systems	wave function	total energies	relative energies ΔE	relative energies ΔH_0[a]
1	MCSCF(10,10)	−155.026 48	0.0	0.0
	MRCI(10,10)	−155.165 16	0.0	0.0
	PT2F(10,10)	−155.576 30	0.0	0.0
2	MCSCF(10,10)	−154.94551	50.8	47.2
	MRCI(10,10)	−155.07963	53.7	50.1
	PT2F	−155.49495	51.0	47.4
5	MCSCF(10,10)	−154.94681	50.0	47.6
	MRCI(10,10)	−155.07910	54.0	51.6
	PT2F	−155.49423	51.5	49.1
6	MCSCF(10,10)	−154.94544	50.8	47.3
	MRCI(10,10)	−155.07884	54.2	50.7
	PT2F	−155.49452	51.3	47.8

[a] Including zero point vibrational energies.

50.2 and 48.2 kcal/mol, respectively. MRCI(10,10) and PT2F calculations with the larger 6-311G(d,p) basis set reduce the barrier to 50.1 and 47.4 kcal/mol, respectively (see Tables 2 and 3). Note that the barrier of 46.1 kcal/mol obtained from an MCSCF(10,10) single point energy at the GVB-P(5) geometry (MCSCF(10,10)//GVB-P(5)) is in excellent agreement with the MCSCF(10,10)//MCSCF(10,10) barrier (see Table 2).

Inversion of bicyclobutane via a bond stretched isomer (**5**) is another possible route. The primary difference between structures **2** and **5**, in addition to the longer C_1C_2 distance in **5** (Table I), is in the staggered, nonplanar arrangement of the hydrogens in the minimum **5**. A transition state (**6**) with C_s symmetry is found to have a long C_1–C_2 bridgehead bond and a C_3–C_1–C_2–C_4 dihedral angle near 180°. This structure has two bridgehead hydrogen and carbon

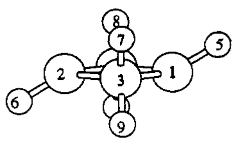

5 C_{2h}

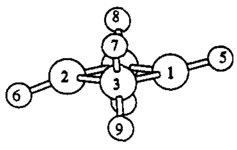

6 C_s

Table 4. MCSCF(10,10), GVB-P(5) (in parentheses), and GVB-P(1) (in brackets) Geometrical Parameters of Bicyclodiazoxane Short (**3**), Long (**4**), and the Isomerization Transition State (**7**), Calculated with the 6-31G(d) Basis Set

system	symetry	bond length N–N	bond length N–O	angle (deg) N–O–N	angle (deg) O–N–O	dihedral angle (deg) O–N–N–O
3	C_{2v}	**1.395**	**1.484**	**56.1**	**90.4**	**107.0**
		(1.367)	(1.484)	(54.9)	(90.4)	(106.2)
		[1.377]	[1.399]	[59.0]	[90.6]	[109.5]
4	D_{2h}	**1.970**	**1.365**	**92.4**	**87.6**	**0.0**
		(1.963)	(1.362)	(92.2)	(87.8)	(0.0)
		[1.908]	[1.324]	[92.3]	[87.7]	[0.0]
7	C_{2v}	**1.893**	**1.469**	**80.2**	**88.7**	**132.2**
		(1.849)	(1.465)	(78.3)	(88.0)	(127.2)
		[1.757]	[1.397]	[77.9]	[88.7]	[128.1]

atoms lying in the σ_h plane (contains H_6, C_2, C_1, and H_5) and an MCSCF(10,10) imaginary frequency of 280i cm^{-1}. The GVB levels of theory also predict **6** to be a transition state. The normal mode corresponding to the MCSCF(10,10) imaginary frequency is displayed in Figure 1b (the GVB normal modes are very similar). The IRC displayed in Figure 2b connects the shallow minimum **5**, via a small barrier **6**, with bicyclobutane (**1**). Initially, descending from the transition state (**6**) involves upward bending of one bridgehead hydrogen (H_6). This is followed by synchrous bending of the two bridgehead hydrogens and two peripheral carbons similar to the inversion IRC discussed above. The MCSCF(10,10)/6-31G(d) bond stretch transition state (**6**) lies 47.0 kcal/mol above bicyclobutane, only 0.2 kcal/mol higher than the inversion barrier (**2**). Since the bond stretch intermediate (**5**) is lower than **6** by less than 1 kcal/mol (0.8 and 0.2 kcal/mol with and without zero point correction, respectively), inversion of bicyclobutane via this two-step mechanism may be competitive. A single point correction with MRCI(10,10) (PT2F) increases the bond stretch barrier (**1** ↔ **6**) to 54.3 (48.5) kcal/mol, only 0.2 (0.2) kcal/mol above (below) the intermediate **5** prior to the addition of zero point corrections. With zero point corrections, the transition state **6** actually falls to 0.8 (1.3) kcal/mol *below* **5** at the MRCI (PT2F) level of theory. Changes in the MRCI and PT2F barrier **6** (and relative energies of **5**) are less than 1 kcal/mol upon going from the 6-31G(d) to 6-311G(d,p) basis set

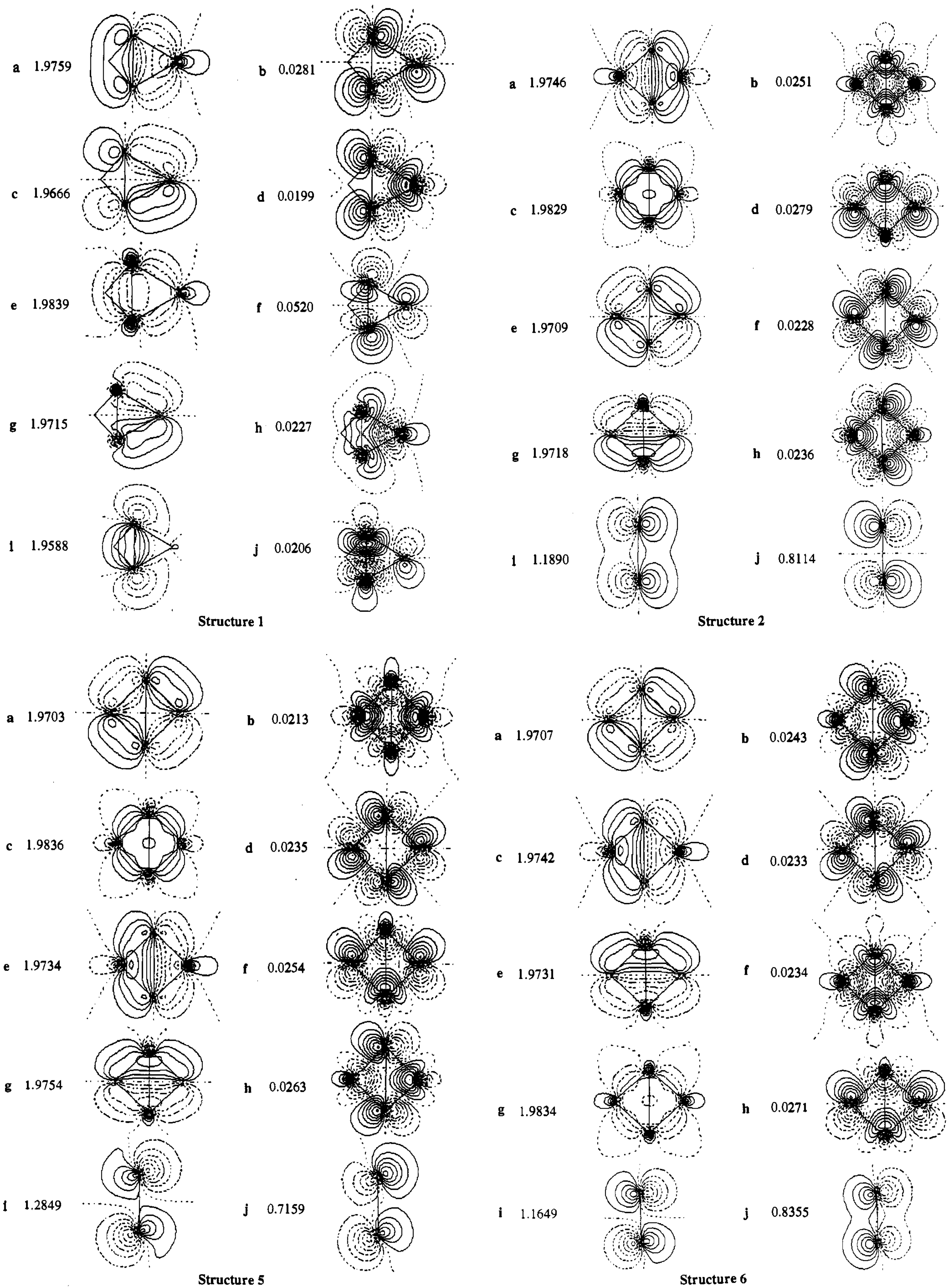

Figure 3. Contour plots of the bicyclobutane correlated reaction orbitals of the optimized MCSCF(10,10)/6-31G(d) wave function in the planes that are made up by two bridgehead atoms and one of two peripheral atoms (numerical values = occupation numbers) for **1**, in the $\sigma_h(xy)$ (**a**–h) and $\sigma_v(yz)$ (**i**, **j**) planes (numerical values = occupation numbers) for **2**, in the YZ (**a**–h) and $\sigma_h(x,y)$ (**i**, **j**) planes (numerical values = occupation numbers) for **9**, and in the $\sigma_h(xy)$ plane (**i**, **j**) and in the planes (**a**–**h**) that are made up by two bridgehead atoms and one of two peripheral atoms (numerical values = occupation numbers) for **6**.

Table 5. 6-31G(d) Total (au) and Relative Energies (kcal/mol^{-1}) of N_2O_2 Systems[a]

systems	wave function	total energies	relative energies ΔE	relative energies ΔH_0[b]
3	GVB-P(1)//GVB-P(1)	−258.319 83 (8.6)	0.0	0.0
	MRCI//GVB-P(1)	−259.070 37	0.0	0.0
	GVB-P(5)//GVB-P(5)	−258.459 66 (6.3)	0.0	0.0
	MCSCF(10,10)//GVB-P(5)	−258.533 67	0.0	0.0
	MCSCF(10,10)//MCSCF(10,10)	−258.534 18 (7.1)	0.0	0.0
	MCSCF(14,12)//MCSCF(10,10)	−258.549 73	0.0	0.0
	MCSCF(18,14)//MCSCF(10,10)	−258.565 89	0.0	0.0
	MRCI(10,10)//MCSCF(10,10)	−258.644 61	0.0	0.0
	PT2F//MCSCF(10,10)	−259.012 46	0.0	0.0
4	GVB-P(1)//GVB-P(1)	−258.379 43 (10.3)	−37.4	−35.7
	MRCI//GVB-P(1)	−259.119 96	−31.1	−29.4
	GVB-P(5)//GVB-P(5)	−258.481 13 (8.8)	−13.5	−13.3
	MCSCF(10,10)//GVB-P(5)	−258.536 80	−2.0	0.5
	MCSCF(10,10)//MCSCF(10,10)	−258.536 84 (8.6)	−1.7	−0.2
	MCSCF(14,12)//MCSCF(10,10)	−258.595 27	−28.6	−27.1
	MCSCF(18,14)//MCSCF(10,10)	−258.557 21	5.4	6.9
	MRCI(10,10)//MCSCF(10,10)	−258.643 73	0.5	2.0
	PT2F//MCSCF(10,10)	−259.06004	−29.9	−28.4
7	GVB-P(1)//GVB-P(1)	−258.284 64 (7.3)	22.1	20.9
	MRCI//GVB-P(1)	−259.022 01	30.3	29.1
	GVB-P(5)//GVB-P(5)	−258.410 31 (5.7)	31.0	30.4
	MCSCF(10,10)//GVB-P(5)	−258.468 57	40.9	40.3
	MCSCF(10,10)//MCSCF(10,10)	−258.465 38 (5.7)	43.2	41.8
	MCSCF(14,12)//MCSCF(10,10)	−258.494 94	34.4	33.0
	MCSCF(18,14)//MCSCF(10,10)	−258.510 16	35.0	33.6
	MRCI(10,10)//MCSCF(10,10)	−258.576 20	42.9	41.5
	PT2F//MCSCF(10,10)	−258.957 39	34.6	33.2

[a] Zero point energies in parentheses. [b] Including zero point vibrational energies.

(see Tables 2 and 3). This again illustrates the flatness of this part of the potential energy surface. The key point is that **2**, **5**, and **6** have very similar energies at the MCSCF, MRCI, and PT2 levels of theory.

The bridgehead C_1–C_2 bond length at the global bicyclobutane minimum **1** is a "normal" 1.504 Å as noted in earlier papers.[3b,8] In contrast, the value of C_1–C_2 is greater than 2 Å in structures **2**, **5**, and **6**, suggesting significant configurational mixing. The amount of configurational mixing in the transition region may be assessed by examining the natural orbital occupation numbers (NOON's) of the various multiconfigurational wave functions. For RHF wave functions, the NOON's are 2 for occupied orbitals and 0 for virtual orbitals. The deviations from these values in multiconfigurational wave functions may therefore be taken as a measure of "diradical character".

The MCSCF(10,10) natural orbitals (NO's) are displayed in Figure 3 for each of the four structures of interest. The orbitals labeled i and j correspond to the C_1–C_2 bridge bond and are the HOMO and LUMO in the RHF and GVB-P(1) wave functions. The NOON's for these NO's are close to 2.0 and 0.0, respectively, in structure **1**, but become nearly 1.0 (true diradicals) in structures **2**, **5**, and **6**. This strong diradical character was noted in the earlier reports by Gassman et al.[3b] and by Schleyer and co-workers,[8] based on small basis set GVB calculations. It is clear from these results that single-configuration-based methods cannot properly account for the bicyclobutane inversion process in a qualitative manner. Attempts to correct the single configuration results with MP2 or CISD apparently provide little improvement.[10b]

The remaining eight NO's displayed in Figure 3 correspond to the four bridgehead peripheral (C_1–C_3, C_1–C_4, C_2–C_3, C_2–C_4) bonds in bicyclobutane. These NO's remain nearly closed shell in nature throughout the inversion process.

2. Bicyclodiazoxane. Like silabicyclobutane,[29] bicyclodiazoxane (**3**) has a bond stretch isomer (**4**). The geometrical parameters of bicyclodiazoxane (**3**), its long bond isomer (**4**), and the transition state (**7**) connecting them are listed in Table 4. At all three [GVB-P(1), GVB-P(5), and MCSCF(10,10)] levels of theory, both isomers are minima on the potential energy surface. The C_{2v} bicyclodiazoxane structure possesses an N–N bond [1.377 Å at MCSCF(10,10)] that is shorter than the N–N single bond in hydrazine [1.447 Å (experiment)] and somewhat longer than the N═N double bond in HN═NH (experimentally determined to be 1.252 Å).[30] The MCSCF(10,10)/6-31G(d) N–O distance of 1.484 Å in **3** is similar to the experimentally determined N–O distance of 1.453 Å[30] in H_2N–OH.

At the MCSCF(10,10)/6-31G(d) level of theory, the planar structure (**4**) with D_{2h} symmetry possesses a much longer N–N distance of 1.970 Å; this is accompanied by a shorter N–O distance (1.365 Å). Similar to bicyclobutane, the large N–N bridgehead distance in **4** suggests significant configurational mixing (Figure 4). The bonding and antibonding NN orbitals (**g** and **h** in Figure 4b) have NOON values of 1.8051 and 0.1945, respectively, for this isomer. In contrast, the values in **3** are 1.9600 and 0.0405, respectively (**i** and **j** for **3** in Figure 4). Note also the qualitative difference in these two orbitals upon stretching the NN bond from **3** to **4**.

The bond stretch transition state (**7**) connecting **3** and **4** has a long N–N bond distance. At the MCSCF(10,10) level of theory, the N–N distance in this transition state structure lengthens to 1.893 Å, 0.498 Å longer than the N–N distance in bicyclodiazoxane (**3**) and only 0.077 Å shorter than the N–N bond in the long bond (**4**) bicyclodiazoxane; however, the 132.2° O–N–N–O dihedral angle of the transition state remains closer to that of bicyclodiazoxane (107.0°) (**3**). As expected, the long N–N distance in the transition state signifies large configurational mixing as shown by the MCSCF NOON's listed for **7** in Figure 4. The N–N bonding (**i**) and antibonding (**j**) orbitals fo the MCSCF(10,10)/6-31G(d) wave function have NOON's of 1.2671 and 0.7340, respectively (see Figure 4, orbitals for **7**).

Inspecting the natural orbitals (see Figure 4, **3**, **4**, **7**) reveals interesting features of the bonding in reactant, transition state and product. Note that the N–N bonding and antibonding orbitals of **3** (**i** and **j**) are σ-like, confirming the normal single N–N bond.

(29) Boatz, J. A.; Gordon, M. S. *J. Phys. Chem.* **1988**, *92*, 3037.

(30) Harmony, M. D.; Laurie, V. W.; Kuczkowski, R. L.; Schwendeman, R. H.; Ramsay, D. A.; Lovas, F. J.; Lafferty, W. J.; Maki, A. G. *J. Phys. Chem. Ref. Data* **1979**, *8*, 619.

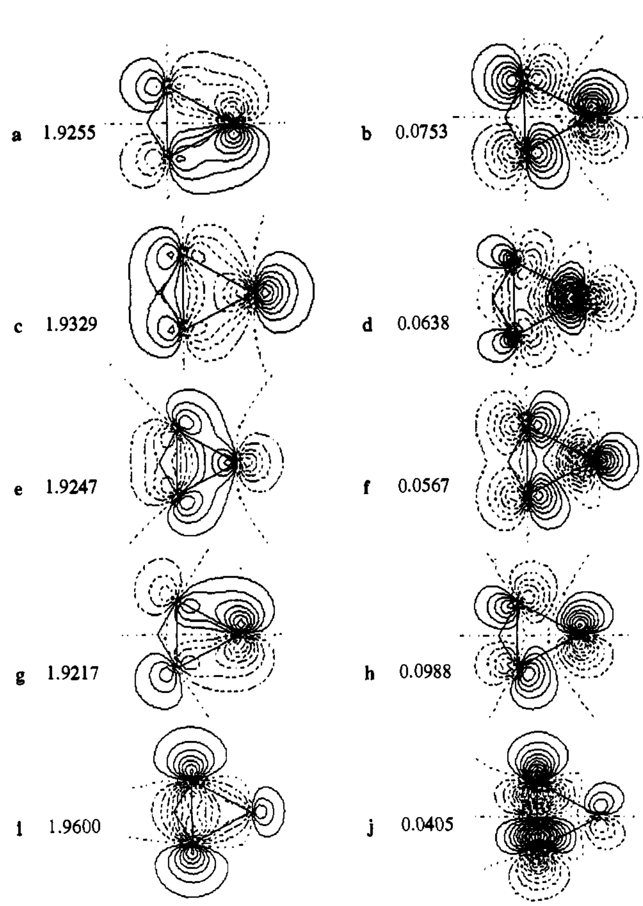

Structure 3

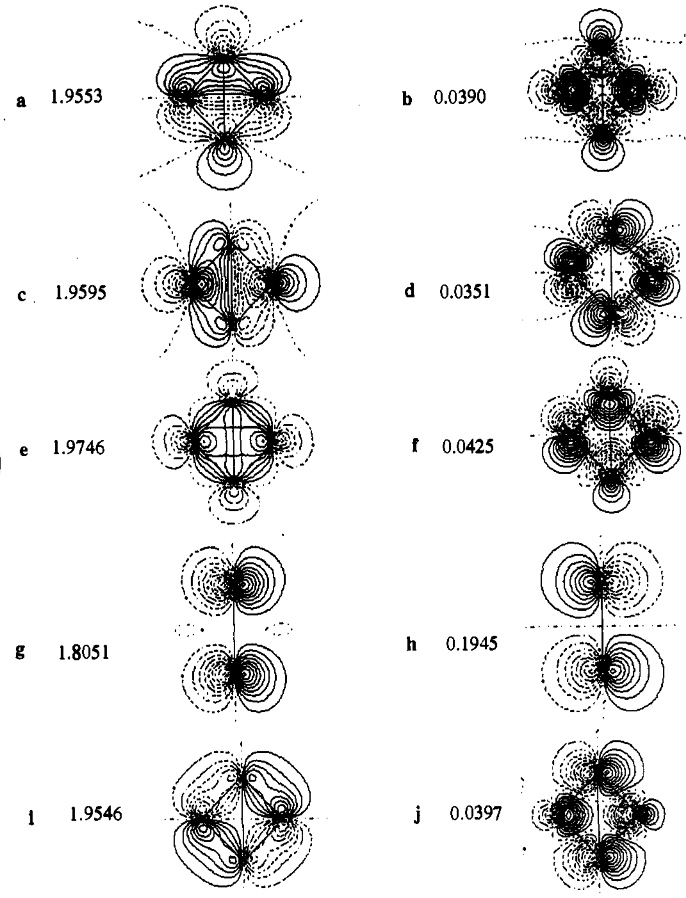

Structure 4

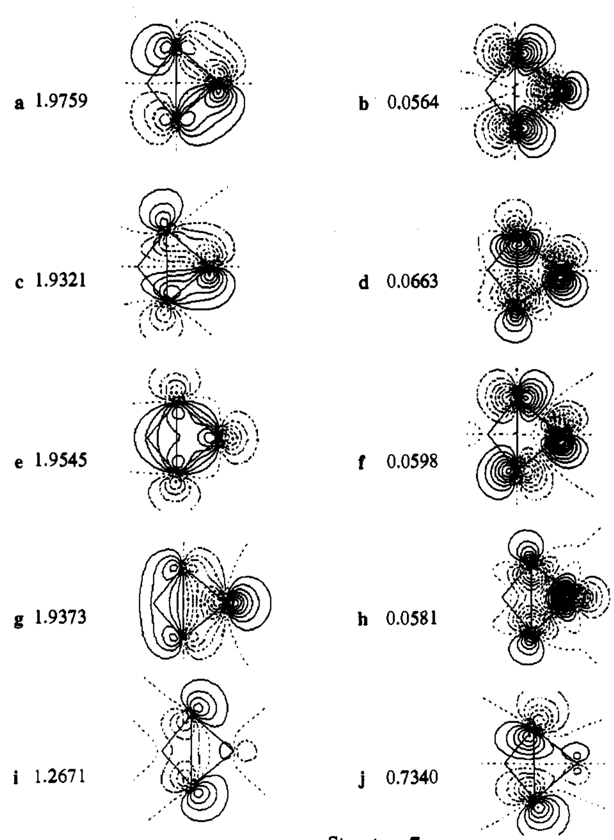

Structure 7

Figure 4. Correlated orbitals of the optimized (10,10) MCSCF/6-31G(d) wave function in the planes containing two bridgehead nitrogen atoms and one of two peripheral oxygen atoms (numerical values = occupation numbers) for **3**, correlated reaction orbitals of the optimized (10,10) MCSCF/6-31G(d) wave function in the $\sigma_h(xy)$ (**a–f, i, j**) and $\sigma_v(xz)$ (**g**, h) planes (numerical values = occupation numbers) for **4**, and contour plots of the correlated reaction orbitals of the optimized MCSCF(10,10)/6-31G(d) wave function in the planes that are made up by two bridgehead atoms and one of two peripheral atoms (numerical value = occupation numbers) for **7**.

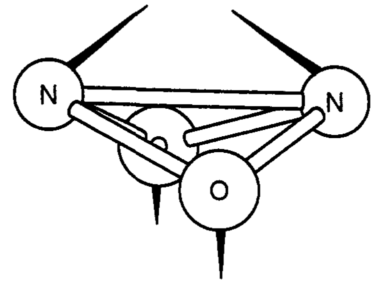

7

Figure 5. MCSCF(10,10)/6-31G(d) imaginary normal mode (1150i cm^{-1}) for 7.

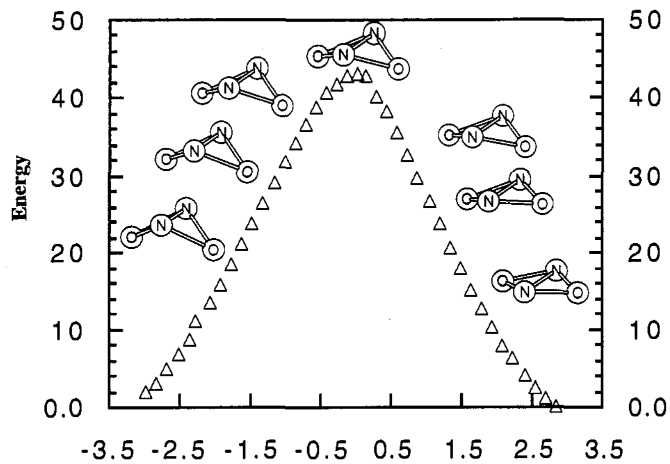

Figure 6. Bicyclodiazoxane bond stretch IRC calculated with MCSCF-(10,10)/6-31G(d); energy in kcal/mol, *s* in $amu^{1/2}$·bohr. The structures displayed along the IRC are of the transition state (top), points 5, 10, and 16 in the forward and reverse directions.

Since the O–N–N–O dihedral angle of bicyclodiazoxane (**3**) is flattened from 107.0° to 180° to form the long bond isomer (**4**) with a much longer N–N bond, the bonding and antibonding orbitals corresponding to the stretched N–N bond become π-like as shown in Figure 4 (**4**, **g** and **h**). In the planar arrangement of **4**, a π lone pair on each oxygen can participate in the bonding to provide extra stability for this 6π-electron system.[31] The differences in bonding between bicyclodiazoxane and the inversion transition state (**4**) are more subtle. While the N–N bonding and antibonding MOs are in transition from σ to π type, the N–O bonding MO's in the transition state (**7**) structure resemble those of bicyclodiazoxane. Although the N_2O_2 natural orbitals are qualitatively similar to those in bicyclobutane, there are significant differences. Whereas bicyclobutane is essentially a pure diradical in its transition state region, the diradical character is much smaller in **7**, though still significant.

It is clear from the MCSCF(10,10) imaginary normal mode (1150i cm^{-1}) of the bond stretch transition state (**7**) displayed in Figure 5 that **7** connects isomers **3** and **4**. An intrinsic reaction coordinate (IRC) traced from **7** to both **3** and **4**—by following the path of steepest descents starting at the transition state (**7**)—verified that **3** connects **4** via **7**. The MCSCF(10,10)/6-31G(d) energy at each point on the IRC is displayed in Figure 6.

The total and relative energies for the N_2O_2 structures are listed in Tables 5 and 6, using the 6-31G(d) and 6-31+G(2d) basis sets, respectively. It is interesting that all levels of theory predict that the stability of isomer **4** is competitive with that of isomer **3**, even though the long N–N distance and the diradical character discussed above suggest the N–N bond is at least partially broken. The MCSCF(10,10) level of theory predicts the two isomers to be similar in energy, and the MRCI(10,10) energies based on this MCSCF(10,10) wave function have little effect on this result.

(31) Zandwijk, v. G.; Janssen, R. A. J.; Buck, H. M. A. *J. Am. Chem. Soc.* **1990**, *112*, 4155.

Table 6. 6-311+G(2d)//MCSCF(10,10)/6-31G(d) Total (au) and Relative Energies (kcal/mol^{-1}) of N_2O_2 Systems

systems	wave function	total energies	relative energies ΔE	relative energies ΔH_0[a]
3	MCSCF(10,10)	−258.614 22	0.0	0.0
	MRCI(10,10)	−258.743 45	0.0	0.0
	PT2F	−259.270 59	0.0	0.0
4	MCSCF(10,10)	−258.619 49	−3.3	−1.8
	MRCI(10,10)	−258.747 44	2.5	−1.0
	PT2F	−259.319 99	−31.0	−29.5
7	MCSCF(10,10)	−258.547 07	42.1	40.7
	MRCI(10,10)	−258.677 12	41.6	40.2
	PT2F	−258.957 39	33.2	31.8

[a] Including zero point vibrational energies.

The most striking result in Tables 5 and 6 is that the PT2F calculations predict a much greater stability for **4** than do the MCSCF(10,10) or the corresponding MRCI results: For the same basis set and size of the active space, PT2F predicts **4** to be nearly 30 kcal/mol more stable than **3**. The primary difference between the internally contracted MRCI(10,10) and PT2F for a given basis set is that whereas the MRCI(10,10) wave function simply includes contractions of single and double excitations of all active orbitals from the configurations generated by the (10,-10) active space, PT2F correlates *all* valence orbitals. In effect, PT2F includes all valence orbitals in the dynamic correlation. The fact that this makes a very large difference for N_2O_2 and virtually no difference for bicyclobutane suggests that the oxygen π lone pairs mentioned earlier play an important role in stabilizing **4**. To explore this possibility, the MCSCF(10,10) active space was expanded to (1) MCSCF(18,14) by adding all the lone pairs except for the π lone pairs on the oxygens and to (2) MCSCF-(14,12) by adding the π lone pairs on each O, since these are most likely to interact with the π system in **4**. As seen in Table 5, this expanded active space brings the MCSCF relative energies in close agreement with the PT2F results while the MCSCF(18,14) is in closer agreement with MCSCF(10,10). Unfortunately, we are unable to perform the full valence MCSCF and MRCI calculation from the MCSCF(14,12) and MCSCF(18,14) reference functions. However, based on the results from the smaller active space, the MRCI is unlikely to modify the MCSCF prediction significantly.

With regard to the barrier height (**3** → **4**), the MRCI and MCSCF(10,10) calculations again predict essentially the same barrier of ca. 41 kcal/mol. Both the PT2F and the MCSCF-(14,12) calculations reduce the barrier to ca. 34 kcal/mol, so the effect of the O π lone pairs is much smaller here (ca. 7 kcal/mol) than for the isomerization energy (ca. 30 kcal/mol).

Table 6 lists the MCSCF(10,10), MRCI(10,10), and PT2F total and relative energies for the N_2O_2 structures calculated with the larger 6-311+G(2d) basis set. The effect on relative energies upon going from 6-31G(d) to 6-311+G(2d) is small; the largest deviation is 3 kcal/mol obtained from MRCI(10,10). The PT2F calculations find a 31.8 kcal/mol inversion barrier, with zero point corrections included.

IV. Summary and Conclusion

The inversion process of bicyclobutane and that of its isoelectronic analog bicyclodiazoxane have been examined at several levels of theory. At the highest and most accurate level of theory (PT2F/6-311G(d,p)//MCSCF(10,10)/6-31G(d) and PT2F/6-311+G(2d)//MCSCF(10,10)/6-31G(d) for bicyclobutane and bicyclodiazoxane, respectively), barriers of 47 and 32 kcal/mol are obtained for the inversion of bicyclobutane and bicyclodiazoxane, respectively. Inversion of the latter system follows a two-step process via a D_{2h} bond stretch isomer. The bicyclobutane inversion process involves a transition region which contains three nearly isoenergetic stationary points at about 47–49 kcal/mol above the minimum. The calculated (PT2F) inversion barrier for bicyclobutane is much higher than that observed experimentally for a highly substituted analog. The origin of this difference must be some combination of the difference in substituents and a less than complete atomic basis set.

Relative energies predicted at the GVB levels of theory are unreliable, although the energetics with MCSCF or MRCI wave function at the GVB geometries deviates only slightly from the predicted energetics at MCSCF geometries.

Acknowledgment. This research was supported in part by a grant (90-0052) from the Air Force Office of Scientific Research, under the High Energy Density Materials Initiative, and in part by a grant from the National Science Foundation (CHE-8911911). Calculations described in this work were performed on an IBM RS6000/530 (obtained through an AFOSR grant to M.S.G.) at North Dakota State University, on an IBM RS6000/350 generously provided by Iowa State University, and on the Cray-2 at the National Center for Supercomputing Applications, Champaign, IL.